Enhancing the photocatalytic activity of TiO$_2$ nanocrystalline thin film by doping with SiO$_2$

E. Rahmani [a,*], A. Ahmadpour [a], M. Zebarjad [b]

[a] Department of Chemical Engineering, Ferdowsi University of Mashhad, Mashhad, Iran
[b] Department of Material Engineering, Ferdowsi University of Mashhad, Mashhad, Iran

ARTICLE INFO

ABSTRACT

Nanocrystalline films of TiO$_2$:XSiO$_2$ (X = mol percent) with high photocatalytic activity was prepared on glass substrate via the sol–gel method. The films were subjected to high temperature treatment at 500 °C for growing TiO$_2$ crystals. Energy Dispersive X-ray Spectroscopy (EDS) was used to indicate the elements in the films. The EDS result showed that besides Ti, O and Si elements, there were small amounts of Ca, Na and Mg. X-ray diffraction (XRD) analysis indicated that TiO$_2$:XSiO$_2$ films contain only anatase phase. Scanning electron microscopy (SEM) was used to study the films surface morphology. The TiO$_2$:SiO$_2$ films that were contacted with methyl orange (MO) in the aqueous solution (10 mg L^{-1}) and irradiated with UV showed a high photocatalytic activity. UV spectrophotometry technique was used to monitor the degradation of methyl orange (MO) by the reduction of main absorbance peak at 464 nm. The results showed that complete degradation was achieved after 1.5 h.

1. Introduction

Photocatalysis is the result of interaction of electrons and holes generated in an activated solid (semiconductor) with its surrounding medium (electrolyte) [1–3]. Recently, the application has been focused on purification and treatment of water and air, which are concerned in the protection of environment, such as nature and life space [4–6]. Utilization of conventional powder catalysts results in disadvantages of employing stirring during the reaction and separation after the reaction, but coating the material as a thin film on the substrate can solve these problems [4,5]. Activation is the consequence of light absorption; therefore, electron–hole pairs are formed in the semiconductor that may recombine or participate in reductive and oxidative reactions [1]. Various metal oxide semiconductors such as: TiO$_2$, ZnO, MoO$_3$, CeO$_2$, ZrO$_2$, WO$_3$, α-Fe$_2$O$_3$, and SnO$_2$ are used as catalysts in the photocatalytic reactions [1,7]. Mechanical stability, non-toxicity and high photoactivity of TiO$_2$ are reasons for favorability of this material as a photocatalyst [1]. Various types of TiO$_2$ such as aerosols, aerogels, nanorods, nanotubes, nanocrystals and mesoporous materials that show promising photoreactivity are synthesized in the recent years [8–10]. A more uniform titanium distribution was obtained by doping TiO$_2$ with SiO$_2$, ZrO$_2$ and other metal oxides [6,10]. The

addition of La$_2$O$_3$, CeO$_2$, CuO, Fe$_2$O$_3$, SiO$_2$, or other oxides into anatase TiO$_2$ can improve the thermal stability and prevent the growth of titania grains [8,10]. Researches show that UV irradiated TiO$_2$ could deactivate and kill airborne microorganisms including bacteria and spores [6,9]. TiO$_2$ has been prepared by several techniques such as chemical vapor deposition (CVD), physical vapor deposition (PVD), and magnetron sputtering. But, these techniques are complex and control of conditions is very difficult [1]. The sol–gel method is easier to use and more economic in comparison with the other techniques [1]. In the present study, nanocrystalline thin film of TiO$_2$:SiO$_2$ was prepared by the sol–gel method. The sol–gel process is a wet chemical technique based on the hydrolysis/polycondensation of metal precursors, which leads to a variety of oxide materials. The thin films were prepared and their photocatalytic activities were then measured by the degradation of methyl orange (MO). Also, the effect of SiO$_2$ addition to the matrix of TiO$_2$ on its photocatalytic activity was investigated.

2. Materials and methods

2.1. TiO$_2$:SiO$_2$ film preparation

All chemicals were analytical reagent grade and used directly without any further purification. Double-distilled water was used throughout this study. TiO$_2$ and SiO$_2$ precursors were tetraisopropoxy titanium (TTIP) and tetraethyl orthosilicate (TEOS).

* Corresponding author. Tel.: +98 9177071108; fax: +98 7112275844.
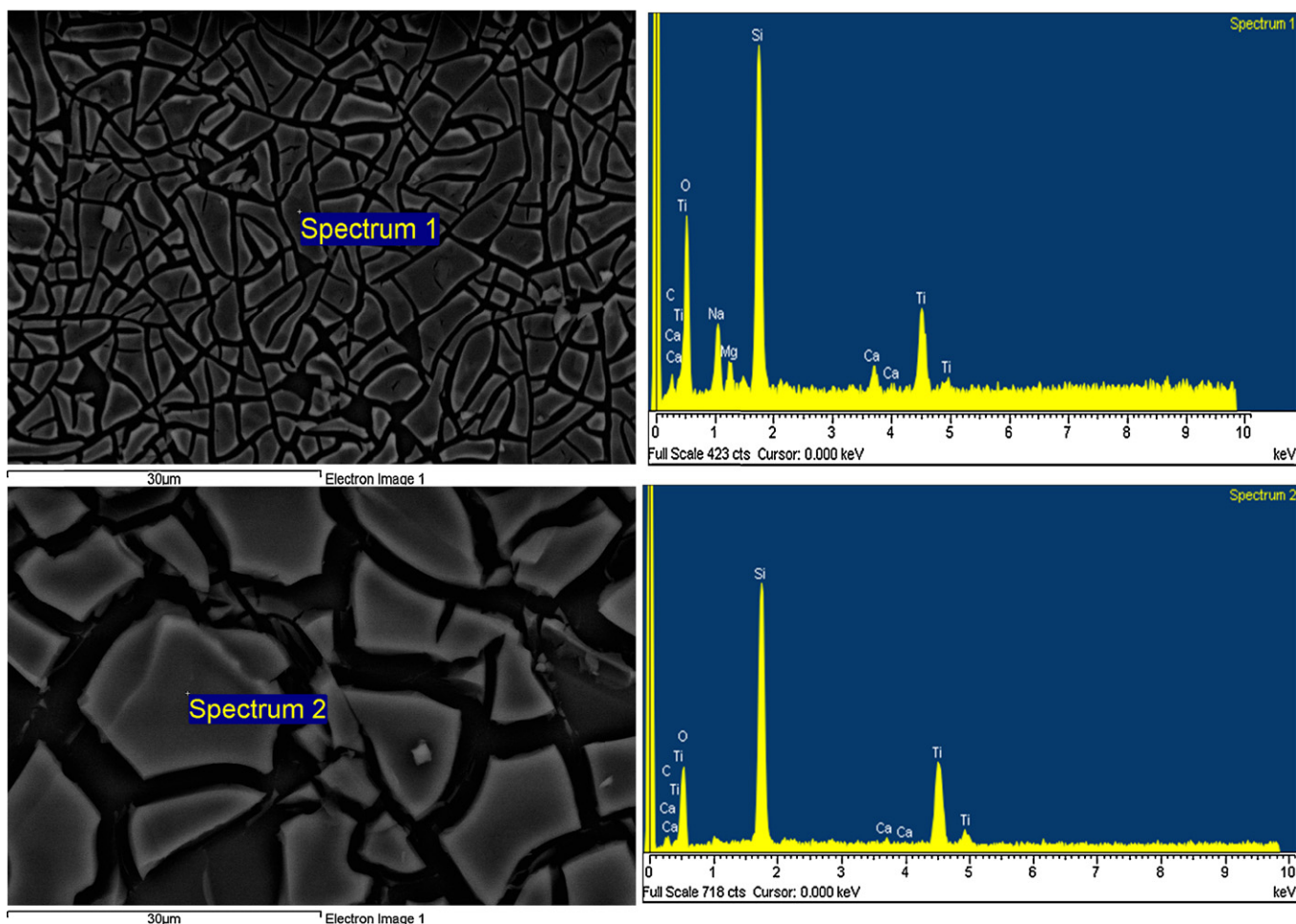E-mail address: ehsanrahmani@hotmail.com (E. Rahmani).

Fig. 1. EDS analyses of the films: spectrum 1 = TiO$_2$, spectrum 2 = TiO$_2$:SiO$_2$.

Ethanol and acetyl acetone (ACAC) were selected as solvent and stabilizer of TTIP [8,11,12].

Nanostructure of TiO$_2$ was prepared by the following method. TEOS (5, 10, and 15 mol percent) was mixed rapidly with 20 mL ethanol for 15 min. Then, the solution was dropped slowly to 67 mL ethanol containing 0.5 mL HCl 1 M and 1 mL deionized water under continuous stirring for 1 h. Meanwhile, TTIP (7 mL) was dissolved into 89.5 mL of ethanol and magnetically stirred for 30 min. Then, ACAC (2 mL) was added to stabilize TTIP solution. The pre-hydrolyzed TEOS solution was poured into the matrix of TiO$_2$ sol and stirred for 30 min. The pure TiO$_2$ film was prepared by the same procedure without adding TEOS. Finally, the sols were aged in a sealed beaker for 24 h. The films were deposited on glass substrates (25 mm × 75 mm × 2 mm) by the dip coating method with a speed of 5 mm s^{-1}, followed by calcinations at 500 °C for 4 h.

2.2. Film characterization

Grain size and crystallinity of the TiO$_2$ films were studied by X-ray diffraction using Cu Kα (λ = 1.5406 Å) radiation in the region of 2θ = 20–75°. In addition, the grain or crystalline size (L) was estimated by Scherrer's formula [1,8] as:

$$L = \frac{k\lambda}{\beta \cos \theta} \tag{1}$$

where L is the crystallite size of pure TiO$_2$, k is a constant (= 0.94), λ is the wavelength of X-ray (Cu Kα = 1.54065 Å), β is the true

half-peak width, and h is the half diffraction angle of the centroid of the peak in degree.

The surface morphology of the films was studied using a Scanning Electron Microscope (SEM, Leo 1450 VP, Zeies, Germany).
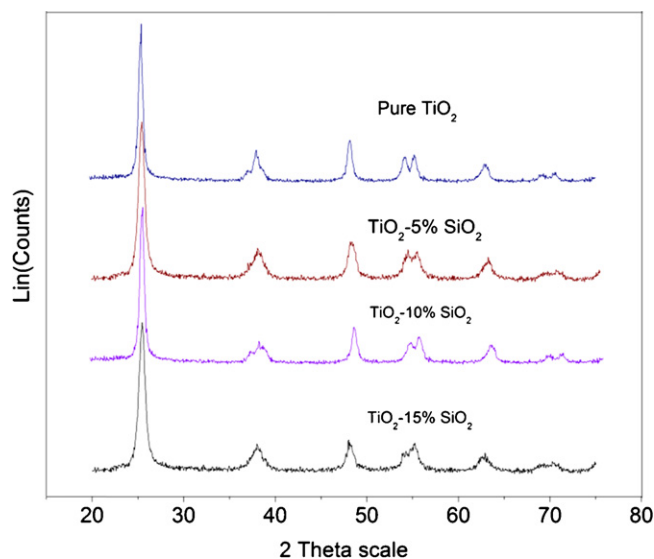

Fig. 2. XRD patterns of the obtained films with different SiO$_2$ content at 500 °C for 4 h.
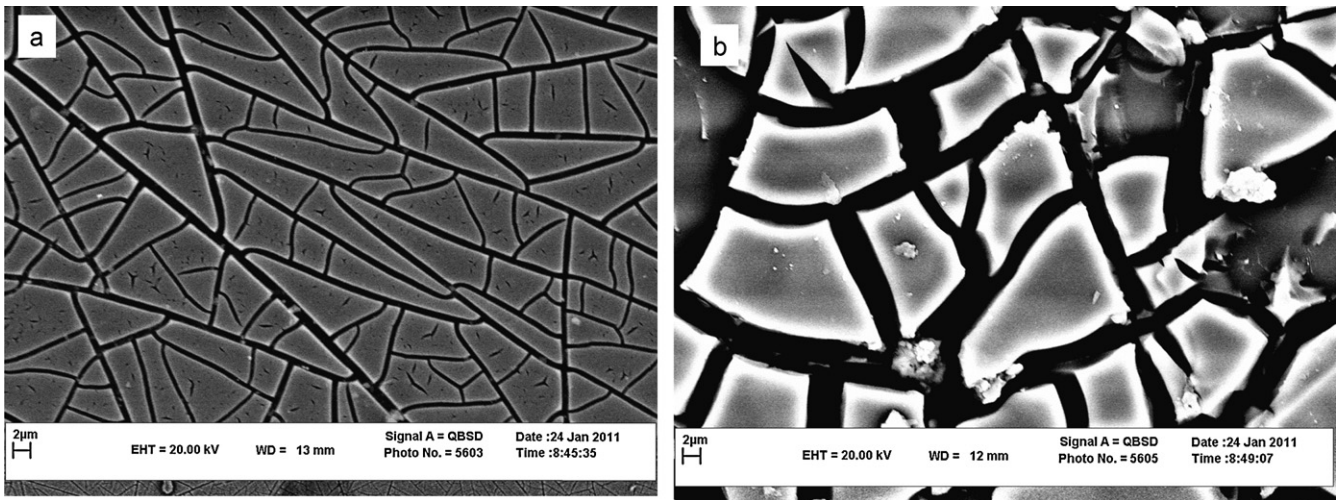
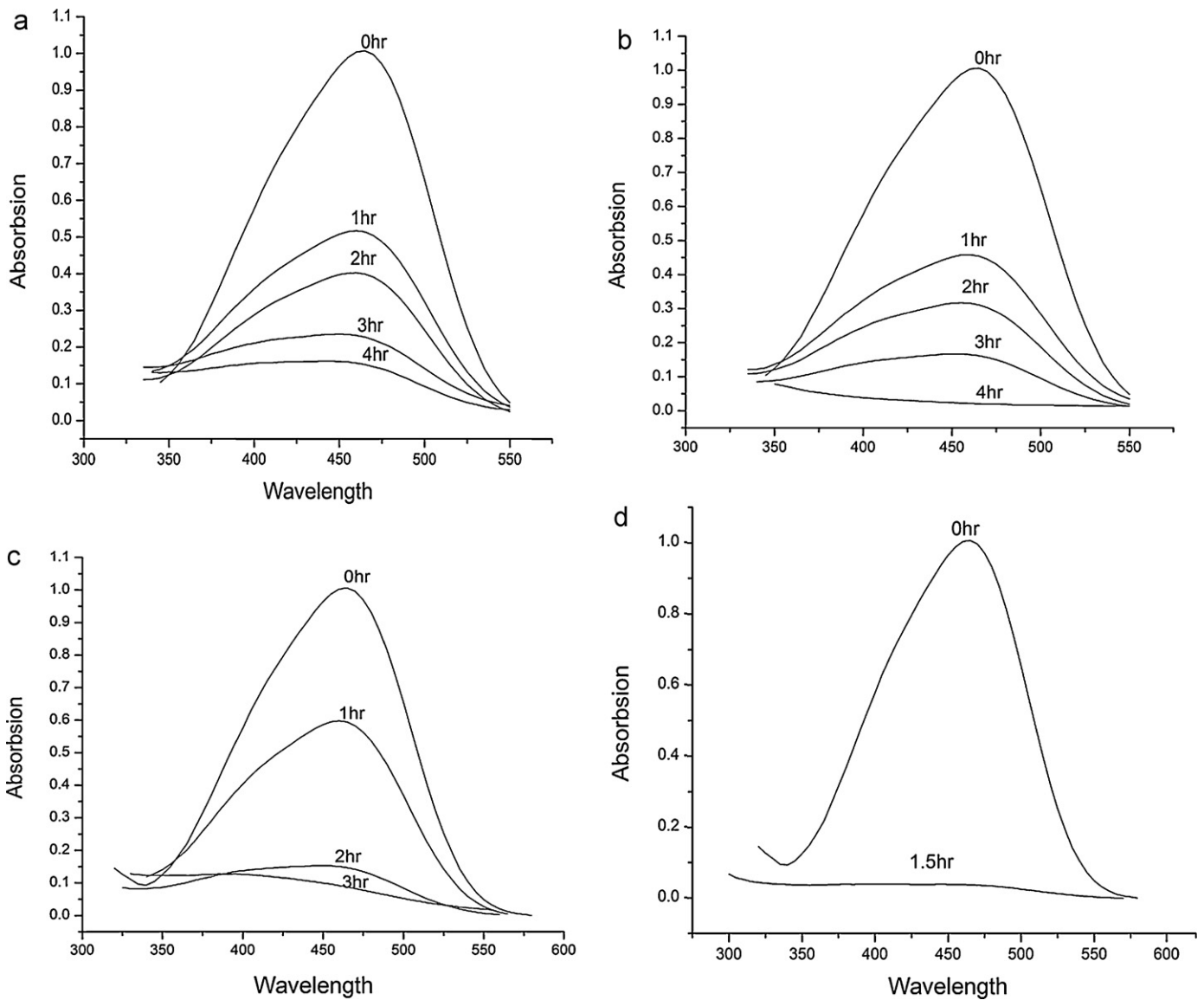**Fig. 3.** SEM images of films: (a) TiO$_2$, (b) TiO$_2$:SiO$_2$.

Fig. 4. Degradation of MO in contact with: (a) Pure TiO$_2$ (b) TiO$_2$–5% SiO$_2$ (c) TiO$_2$–10% SiO$_2$ (d) TiO$_2$–15% SiO$_2$.

Energy Dispersive X-ray Spectroscopy (EDS, 7353, Axford, England) was used for elements analysis.

2.3. Photocatalytic activity measurement

Methyl orange (MO) powder ($C_{14}H_{14}N_3NaO_3S$) dissolved in distilled water at $10\,mg\,L^{-1}$ concentration. The TiO_2 film ($2\,mm \times 2\,mm$) was settled in 5 mL MO solution and a high pressure mercury lamp (125 W) was used as a light source. One face of TiO_2 thin film was irradiated with UV lamp. The averaged intensity of UV irradiance was $6.8\,mW\,cm^{-2}$ by measuring with a UV irradiance meter. The solution was bubbled with air during irradiation. The photocatalytic decolorization of MO is a pseudo-first order reaction and its kinetic may be expressed as follows [5,13]:

$$\ln\left(\frac{C_0}{C}\right) = kt \tag{2}$$

where k is constant rate of reaction, C_0 and C are initial and final concentration of methyl orange. The photocatalytic reaction involves the presence of oxygen and moisture on the photocatalyst surface to activate the photoreaction during light irradiation. From the fundamental photocatalytic kinetics, the reaction equation can be expressed as [13–15]:

$$TiO_2 \rightarrow TiO_2(e^- + h^+) \tag{3}$$

$$O_{2ads} + e^- \rightarrow O_{2ads}{}^- \tag{4}$$

$$H_2O_{ads} + h^+ \rightarrow {}^\bullet OH + H^+ \tag{5}$$

where ads represented the adsorbed state of species on the TiO_2 surface. The mechanism of the photocatalytic reaction can be described as the TiO_2 photocatalyst at first absorbed the light to generate free electron–hole pairs on the TiO_2 surface. The electrons reacted with oxygen to generate superoxide ion (O^{2-}); while the holes redox with H_2O to produce OH radicals [13,14].

3. Results and discussion

3.1. Characterization of the film

Fig. 1 shows the EDS pattern of TiO_2 and $TiO_2:SiO_2$ films. EDS results indicated the main peaks of Ti, Si and also small amounts of Na, Ca, Mg. Presence of Na, Ca and Mg in EDS result is belonging to composition of the glass substrate. Actually these elements existing in glass substrate and X-ray can diffuse over the thickness of the film and detect these elements. Moreover, the presence of SiO_2 in the thin film can destroy the linkage of Ti–O–Ti and change it to Ti–O–Si. This can shift the binding energy of Si to higher value [8].

Fig. 2 shows XRD patterns of thin film at 500 °C. The crystalline size of TiO_2 can be deduced from XRD line broadening using the Scherrer equation [1,8]. Accordingly, the average grain size of TiO_2, TiO_2–5% SiO_2, TiO_2–10% SiO_2 and TiO_2–15% SiO_2 are 33, 19, 15 and 10 nm, respectively. The results indicate that high content of SiO_2 restrain the crystallization of TiO_2 and effectively suppress the phase transformation of TiO_2 from anatase to rutile. This strong retarding has been often ascribed to a good chemical homogeneity of the starting gels, i.e., to a high degree of Si–O–Ti bonding, which is believed to be reason of restricting the growth of grains during heat treatment [8,15–19].

3.2. Surface morphology of $TiO_2:SiO_2$ film

The surface morphology of films can be observed in Fig. 3 which shows SEM micrographs of 10 layers of TiO_2 and $TiO_2:SiO_2$ films. The films produced by this technique indicate fractured morphology. During the drying and annealing processes of the films, crack formation takes place as a result of contraction, stress and different
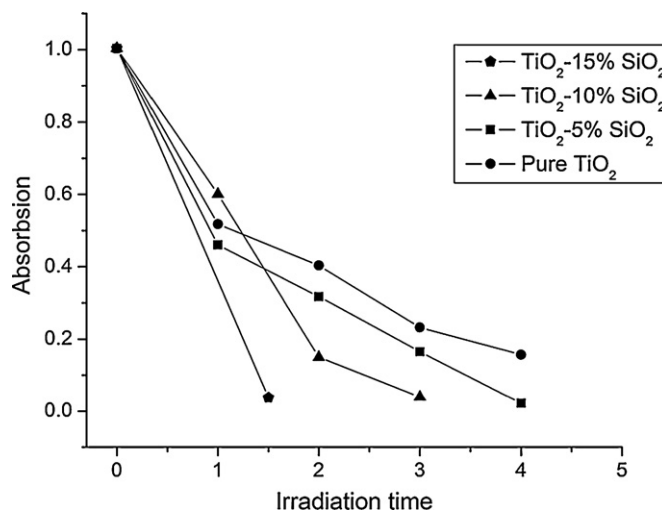

Fig. 5. Concentration of MO in contact with TiO_2, $TiO_2:XSiO_2$ films during the time.

thermal coefficients of expansion of the overlayer and substrate. The fractured surface morphology of the films produced by this technique resulted in a large surface area that would suggest a higher photocatalytic activity. In fact, higher photocatalytic activity with smaller crystalline size of TiO_2 was observed [20].

3.3. Determination of photocatalytic activity of $TiO_2:SiO_2$ films

The photocatalytic activity of the $TiO_2:SiO_2$ films was investigated from the degradation of 5 mL of $10\,mg\,L^{-1}$ MO solution under UV irradiation. Fig. 4 shows degradation of MO solution in contact with $TiO_2:SiO_2$ films under UV irradiation. Fig. 5 also shows change of concentration of MO during irradiation time. A comparison of the photocatalytic activities of four films gives the following order: $TiO_2:15\%\ SiO_2 > TiO_2:10\%\ SiO_2 > TiO_2:5\%\ SiO_2 > TiO_2$. We have calculated constant rate k (min^{-1}) for photodegradation of methyl orange with Fig. 6 according to Eq. (2) and compared these result with other reported titania–silica system (Table 1, [21]). The lowest degradation rate is shown by pure TiO_2 with $k = 6.93 \times 10^{-3}$, that is because of lower surface area with higher crystalline size. Highest
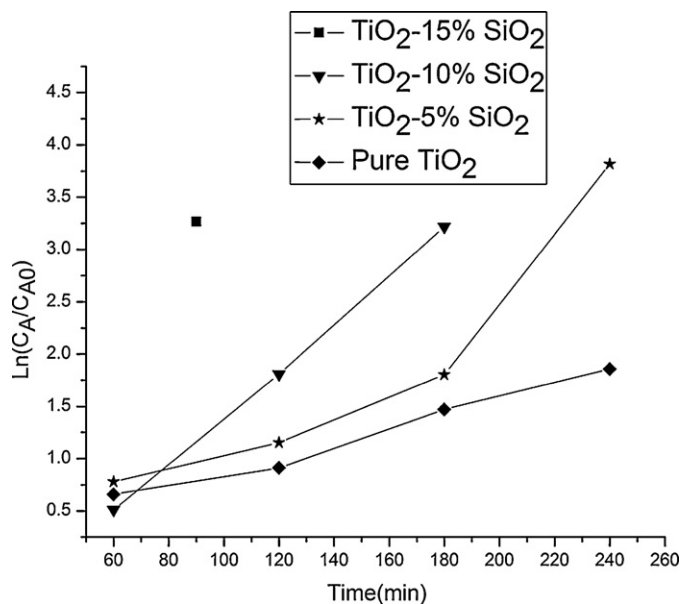

Fig. 6. Evaluation of the rate constants (k) for TiO2, $TiO_2:XSiO_2$.

Table 1
First-order reaction rate constants (k) of different photocatalysts.

Sample type	Dye name	Rate constant k (min^{-1})	Reference
Ti-SBA-15 (sample 1)	Methylene blue	4.70×10^{-2}	[21]
Ti-SBA-15 (sample 2)	Methylene blue	3.80×10^{-2}	[21]
TiO_2:15% SiO_2	Methyl orange	3.63×10^{-2}	This Work
TiO_2:10% SiO_2	Methyl orange	2.26×10^{-2}	This Work
TiO_2:5% SiO_2	Methyl orange	1.63×10^{-2}	This Work
Pure TiO_2	Methyl orange	6.93×10^{-2}	This Work

degradation rate was shown by $TiO_2–15\%$ SiO_2 with $k = 3.63 \times 10^{-2}$ but mole percent of Si must be in an optimal value because in high mole percent of SiO_2, crystals of TiO_2 cannot grow and photocatalytic activity is very low.

The photocatalytic activity of TiO_2:SiO_2 films and powder suspensions is primarily attributed to the surface area of the catalyst. In the case of TiO_2 film, the surface area depends on TiO_2 particle size and substrate. This could be explained by the formation of film with higher total surface area as a result of fractured surface morphology and exposed sublayers as discussed in the SEM analysis (Fig. 3). On the other hand, higher photocatalytic activity was shown by the films produced by smaller TiO_2 crystals.

4. Conclusions

TiO_2:SiO_2 films with high photocatalytic activity were prepared on glass substrate with the sol–gel method using TiO_2 solution from TTIP with different mole percent of SiO_2 where the TEOS was source of SiO_2. XRD patterns indicate that with higher mole percent of SiO_2, the TiO_2 grain size becomes smaller, therefore TiO_2 crystallines have more active surface area and this can enhance the photocatalytic activity of TiO_2. The SEM image illustrated the fractured morphology and sublayers exposed by micro-fractures in the final layer which contribute to larger total surface area and consequently greater photocatalytic activity.

References

[1] L. Lopez, W.A. Daoud, D. Dutta, J. Surf. Coat. Technol. 205 (2010) 251–257.
[2] J.H. Xin, S.M. Zhang, G.D. Qi, X.C. Zheng, W.P. Huang, S.H. Wu, J. React. Kinet. Catal. Lett. 2 (2005) 291–298.
[3] K. Hashimoto, H. Irie, A. Fujishima, J. Jpn. Appl. Phys. 12 (2005) 8269–8285.
[4] J. Yu, X. Zhao, Q. Zhao, J. Mater. Chem. Phys. 69 (2001) 25–29.
[5] J. Yu, X. Zhao, Q. Zhao, J. Mater. Sci. Lett. 19 (2000) 1015–1017.
[6] S. Cao, K.L. Yeung, P.L. Yue, J. Appl. Catal. B 68 (2006) 99–108.
[7] C. Shifu, Z. Wei, L. Wei, Z. Sujuan, J. Appl. Surf. Sci. 255 (2008) 2478–2484.
[8] Q. Jia, Y. Zhang, Z. Wu, P. Zhang, J. Tribol. Lett. 1 (2006).
[9] K.L. Yeung, W.K. Leung, N. Yao, S. Cao, J. Cataly. Today 143 (2009) 218–224.
[10] S. Cao, K.L. Yeung, J.K.C. Kwan, P.M.T. To, S.C.T. Yu, J. Appl. Catal. B 86 (2009) 127–136.
[11] W. Zhang, W. Liu, C. Wang, J. Wear 253 (2002) 377–384.
[12] N. Yao, S.l. Cao, K.L. Yeung, J. Micropor. Mesopor. Mater. 117 (2009) 570–579.
[13] C.K. Leo, H. Liau, T.C.K. Chang, C.L. Yang, Huang, J. Chin. Inst. Chem. Eng. 39 (2008) 237–242.
[14] Y. Zhiyong, E. Mielczarski, J.A. Mielczarski, D. Laubc, L. Kiwi-Minsker, A. Renken, J. Kiwi, J. Mol. Catal. A 260 (2006) 227–234.
[15] K.S. Yao, T.C. Cheng, S.J. Li, L.Y. Yang, K.C. Tzeng, C.Y. Chang, Y. Ko, J. Surf. Coat. Technol. 203 (2008) 922–924.
[16] C. He, B. Tian, J. Zhang, J. Colloid Inter. Sci. 344 (2010) 382–389.
[17] S. Mianxin, B. Liang, Z. Tianliang, Z. Xiaoyong, J. Rare Earths 5 (2008) 693.
[18] H. Yamashita, H. Nose, Y. Kuwahara, Y. Nishida, S. Yuan, K. Mori, J. Appl. Catal. A 350 (2008) 164–168.
[19] P. Novotná, J. Žita, J. Krýsa, V. Kalousek, J. Rathouský, J. Appl. Catal. B 79 (2007) 179–185.
[20] M. Bellardita, M. Addamoa, A. Di Paolaa, G. Marcìa, L. Palmisanoa, L. Cassarb, M. Borsac, J. Hazard. Mater. 174 (2010) 707–713.
[21] S.K. Das, M.K. Bhunia, A. Bhaumik, J. Solid State Chem. 183 (2010) 1326–1333.